

# A Facile Method for Reversibly Linking a Recombinant Protein to DNA

Russell P. Goodman,<sup>[a, b]</sup> Christoph M. Erben,<sup>[a]</sup> Jonathan Malo,<sup>[a, c]</sup> Wei M. Ho,<sup>[a]</sup> Mireya L. McKee,<sup>[a]</sup> Achillefs N. Kapanidis,<sup>[a]</sup> and Andrew J. Turberfield<sup>\*[a]</sup>

We present a facile method for linking recombinant proteins to DNA. It is based on the nickel-mediated interaction between a hexahistidine tag (His<sub>6</sub>-tag) and DNA functionalized with three nitrilotriacetic acid (NTA) groups. The resulting DNA–protein linkage is site-specific. It can be broken quickly and con-

trollably by the addition of a chelating agent that binds nickel. We have used this new linker to bind proteins to a variety of DNA motifs commonly used in the fabrication of nanostructures by DNA self-assembly.

## Introduction

Synthetic structures on the nanometre scale can be made quickly and efficiently by self-assembly of DNA oligonucleotides. Incorporation of proteins into these nanostructures is a promising way to increase their functionality: DNA structures have been used to arrange protein molecules in one,<sup>[1]</sup> two<sup>[2]</sup> or three dimensions<sup>[3]</sup> and to encapsulate them.<sup>[4]</sup> Other applications of DNA–protein conjugation include the formation of functional enzyme complexes,<sup>[5]</sup> fluorescence resonance energy transfer (FRET) systems,<sup>[6]</sup> sensitive detection by immuno-PCR<sup>[7]</sup> and the construction of protein or peptide arrays by hybridization to surface-bound DNA probes.<sup>[8]</sup> Several methods for making covalent DNA–protein linkages have been developed, including bifunctional crosslinkers,<sup>[8,9]</sup> disulfide bonds<sup>[10]</sup> and click chemistry.<sup>[3]</sup> A methyltransferase can be used to form an abortive covalent complex with a modified base.<sup>[11]</sup> Cysteine-modified DNA oligomers can be coupled to recombinant intein-fusion proteins by expressed protein ligation.<sup>[12]</sup> Noncovalent interactions can also be used. Protein-binding aptamer domains<sup>[13]</sup> can be incorporated in DNA nanostructures,<sup>[1b,14]</sup> antibodies have been bound to hapten-functionalized DNA,<sup>[15]</sup> and enzymes have been linked to DNA conjugated to a cofactor.<sup>[16]</sup> The vitamin biotin, which can be conjugated to an oligonucleotide, forms a strong and specific bond with femtomolar affinity to the protein streptavidin,<sup>[17]</sup> which can be fused to another protein<sup>[7]</sup> or linked to other biotinylated molecules.<sup>[18]</sup> Herein, we present a new, facile method for noncovalent attachment of recombinant proteins to DNA that is robust, site-specific and reversible. We show that it is generally applicable to the functionalization of synthetic DNA nanostructures.

The linkage is based on the nickel-mediated interaction between nitrilotriacetic acid (NTA) and a protein carrying a hexahistidine tag (His<sub>6</sub>-tag). Two histidines together with one NTA can satisfy all six coordination sites of a nickel(II) ion. A His<sub>6</sub>-tag is often incorporated at the N or C terminus of a recombinant protein, which can then be purified by immobilized metal ion affinity chromatography<sup>[19]</sup> on an NTA-functionalized column. Clustering NTA groups strengthens the interaction.<sup>[20]</sup> Lata

et al. have shown that the linkage between a His<sub>6</sub>-tag and three coupled NTA groups is particularly stable, with a dissociation constant of the order of 10 nM, but can be broken under mild conditions by the addition of a competing nickel chelator.<sup>[21]</sup> We demonstrate the facile synthesis of DNA with three closely spaced NTA modifications and demonstrate that this modification allows us to link His<sub>6</sub>-tagged proteins to a range of DNA nanostructure motifs. This linkage combines many of the advantages of other linkers: the interaction is site-specific and stable but, unlike a covalent bond, it can be easily reversed.

## Results and Discussion

### Analysis of NTA-modified oligonucleotides

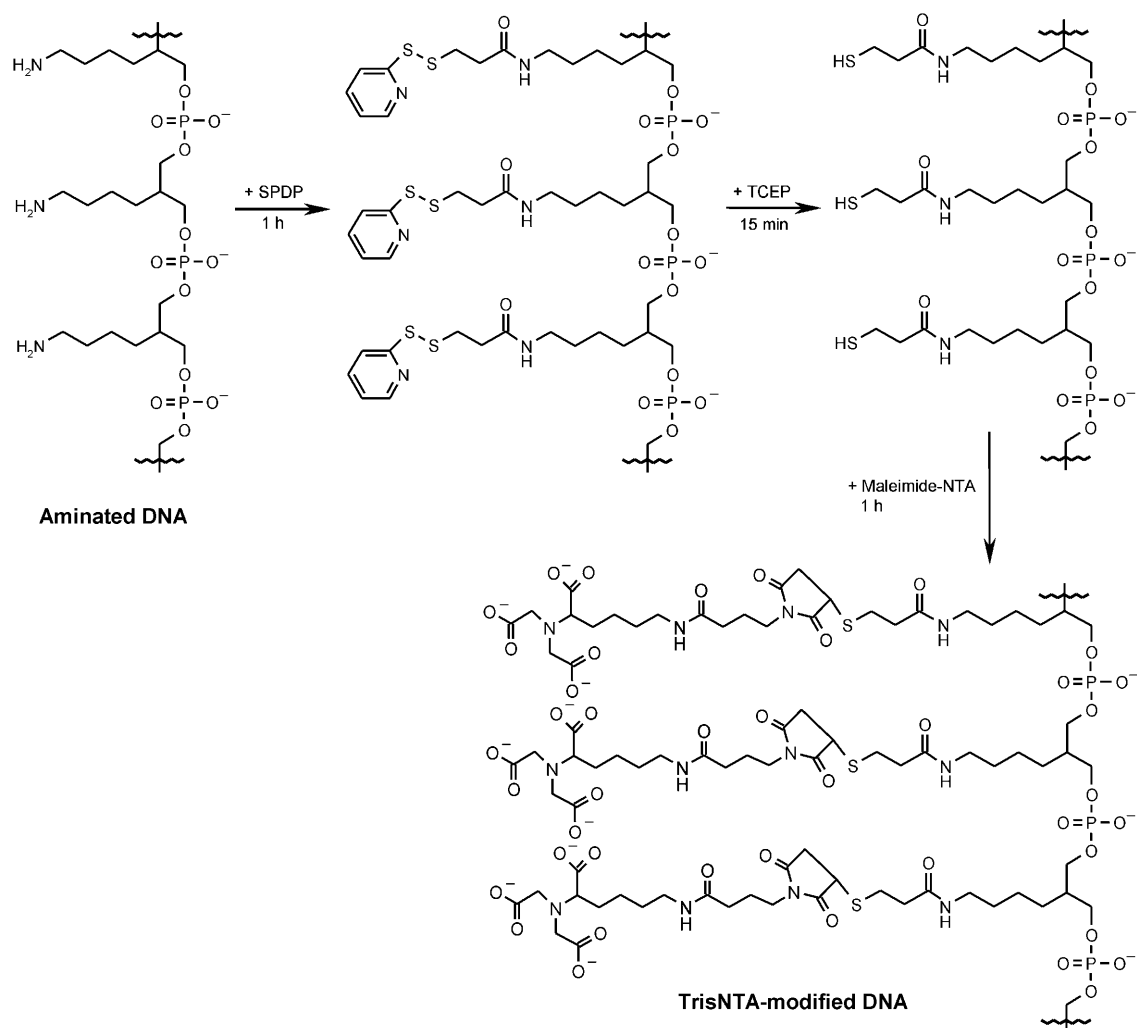
We have prepared DNA oligonucleotides with one, two and three NTA groups (mono-, bis- and trisNTA-functionalized oligonucleotides). The synthesis of trisNTA-modified DNA is illustrated in Scheme 1. An aminated oligonucleotide is treated with the heterobifunctional crosslinker *N*-succinimidyl 3-(2-pyridyldithio)propionate (SPDP). The disulfide bond is then reduced, and the resulting thiol group is treated with maleimide–NTA. Control experiments followed the same protocol

[a] Dr. R. P. Goodman, Dr. C. M. Erben, Dr. J. Malo, W. M. Ho, Dr. M. L. McKee, Dr. A. N. Kapanidis, Prof. A. J. Turberfield  
Department of Physics, Clarendon Laboratory, University of Oxford  
Parks Road, Oxford OX1 3PU (UK)  
Fax: (+44) 1865-272400  
E-mail: a.turberfield@physics.ox.ac.uk

[b] Dr. R. P. Goodman  
Present address: William Bosworth Castle Society, Harvard Medical School  
260 Longwood Avenue, Boston, MA 02115 (USA)

[c] Dr. J. Malo  
Present address: St. George's University of London  
Cranmer Terrace, London SW17 0RE (UK)

Supporting information for this article is available on the WWW under <http://dx.doi.org/10.1002/cbic.200900165>.



**Scheme 1.** Synthesis of a DNA oligonucleotide functionalized with three NTA groups (trisNTA).

with a substoichiometric amount of SPDP (molar ratio: ~two amine modifications per SPDP) to create partially NTA-modified oligonucleotides. NTA-functionalized oligonucleotides were purified either by reversed-phase liquid chromatography (RPLC) or by denaturing PAGE purification. The synthesis and purification of mono- and bisNTA-modified DNA starting from oligonucleotides with one or two amine modifications is analogous. (See the Experimental Section for details of syntheses and purification.)

The denaturing PAGE gel in Figure 1 demonstrates the synthesis and purification of mono-, bis- and trisNTA oligonucleotides. The starting materials were 27-mer DNA oligonucleotides ("Oligo 1"; see the Supporting Information for the base sequence) with one, two or three amine modifications at the 5'-end (lanes A1, B1 and C1). Incubation with SPDP leads to a small reduction in mobility (lanes 2), and a disulfide dimer can be seen in lane A2. Lanes 3 contain the control: the product of the full synthesis using a substoichiometric amount of SPDP to generate partially NTA-modified oligonucleotides (for example, lane C3 contains oligonucleotides that carry three amines, but only one or two of them have been converted into NTAs).

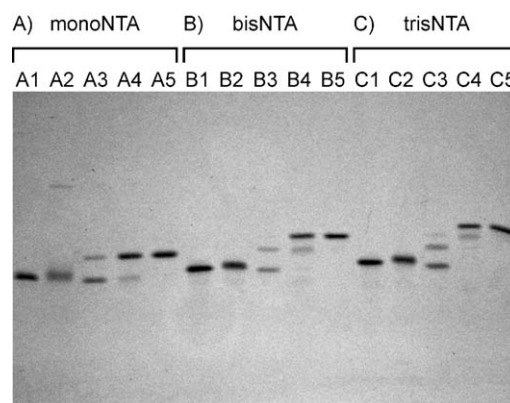


**Figure 1.** Synthesis of A) mono-, B) bis- and C) trisNTA-modified 27-mer DNA oligonucleotides. Lanes 1: Aminated DNA precursor. Lanes 2: Thiol-functionalized DNA after incubation with SPDP. Lanes 3: Reaction of partially thiolated DNA with maleimide-NTA. Lanes 4: Reaction of thiolated DNA with maleimide-NTA. (Note that failure products are evident in each reaction but occur in greater concentration in the case of substoichiometric thiolation.) Lanes 5: Contents of lanes 4 after purification: lane A5: PAGE-purified mono-NTA-DNA, lanes B5 and C5: RPLC-purified bis- and trisNTA-DNA, respectively.

Lanes 4 show the product of synthesis. In each case, the dominant band corresponds to fully NTA-modified oligonucleotides, although partially modified oligonucleotides are also present. The yield for modification of oligo 1 was approximately 71% for monoNTA, 57% for bisNTA and 60% for trisNTA. Purified NTA-oligonucleotides are analysed in lanes A5, B5 and C5: the single bands correspond to the desired monoNTA, bisNTA and trisNTA oligonucleotides, respectively. The identity of the NTA-modified oligonucleotides was also confirmed by mass spectrometry (see Table 1.)

**Table 1.** Mass spectrometry of NTA-modified oligonucleotide "Oligo 1".

Oligo 1 modified with:	Expected mass [Da] <sup>[a]</sup>	Measured mass [Da]
monoNTA	9123.2	9122.4
bisNTA	9848.0	9847.3
trisNTA	10572.6	10572.1

[a] The expected masses assume NTA-modified oligonucleotides with protonated carboxyl groups.

### Size-exclusion chromatography

Binding of single-stranded, NTA-modified DNA to His<sub>6</sub>-tagged green fluorescent protein (GFP) was investigated by size-exclusion liquid chromatography (SEC). The 27-mer "Oligo 1" was modified with mono-, bis- and trisNTA, as described above. The NTA-modified oligonucleotides were diluted to a concentration of 19  $\mu\text{M}$  in 20  $\mu\text{L}$  TN buffer (10 mM Tris, 100 mM NaCl, pH 8) and combined with NiSO<sub>4</sub> (2  $\mu\text{L}$ , 5 mM). After 30 min at room temperature, excess nickel ions were removed by using a gel filtration spin column (Micro Bio-Spin 6; Bio-Rad). His<sub>6</sub>-tagged GFP was added ([GFP]/[DNA] ~ 2:3), and the mixture was incubated for 30 min at room temperature. (One-step incubation of GFP and DNA with a small excess of NiSO<sub>4</sub> for ~1 hour is also effective and removes the need for the gel filtration spin column; data not shown.) The sample was then diluted with TN buffer to give final concentrations of DNA and GFP of ~3  $\mu\text{M}$  and ~2  $\mu\text{M}$ , respectively. 100  $\mu\text{L}$  of this solution was loaded for analysis by SEC.

Figure 2 shows SEC analysis of the products of incubation of mono-, bis- and trisNTA oligonucleotides with His<sub>6</sub>-tagged GFP. Absorbance measurements at 260 and 395 nm, the absorption maximum of the GFP fluorophore,<sup>[22]</sup> indicate the presence of DNA and GFP, respectively. Controls containing purified mono-, bis- and trisNTA oligonucleotides and GFP separately are also shown. Incubation of the monoNTA oligonucleotide with GFP does not result in a significant shift of the DNA peak. Incubation of the bisNTA oligonucleotide with GFP results in a shift of both peaks that is consistent with a transient interaction between the bisNTA oligonucleotide and the protein with a time-scale comparable to that of the experiment (ca. 30 min). Incubation of the trisNTA oligonucleotide with GFP results in a stronger shift of both the DNA and the GFP peaks; both peaks now elute simultaneously at a smaller solvent volume; this is consistent with the formation of a GFP-His<sub>6</sub>:Ni<sup>2+</sup>:trisNTA-DNA complex. The protein peak is entirely shifted to the new posi-

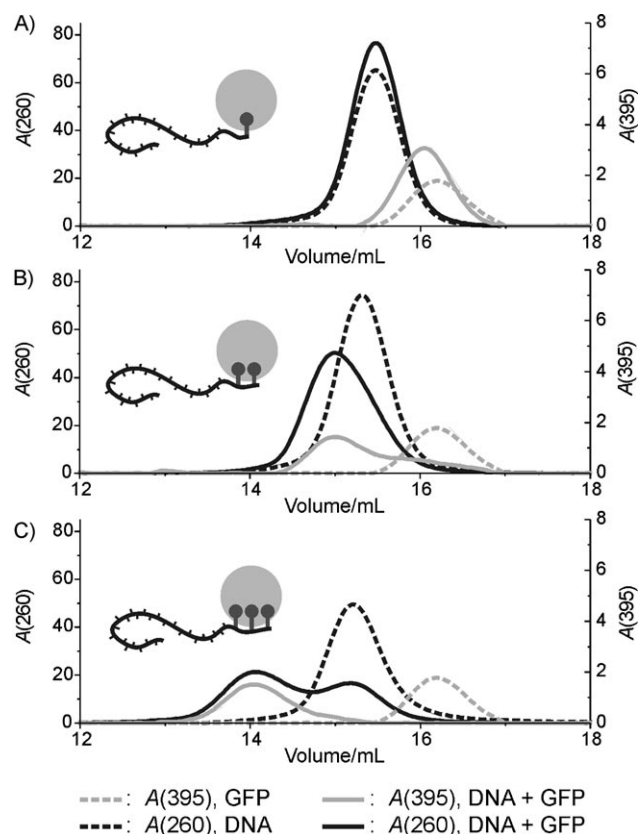


**Figure 2.** Analysis of binding between NTA-modified DNA and His<sub>6</sub>-tagged GFP by SEC. Elution of DNA oligonucleotides and of GFP from the SEC column was monitored by measuring absorbance at 260 nm (left vertical axis, black lines) and 395 nm (right vertical axis, grey lines), respectively. SEC traces of: A) mono-, B) bis- and C) trisNTA-functionalized DNA oligonucleotides (27-mer) after incubation with NiSO<sub>4</sub> and His<sub>6</sub>-tagged GFP (solid lines). Controls: NTA-functionalized oligonucleotides only (dotted black lines); His<sub>6</sub>-tagged GFP only (dotted grey lines).

tion; excess DNA remains unbound. We conclude that the strength of binding increases in the order monoNTA < bisNTA < trisNTA.

In order to demonstrate the use of trisNTA to bind proteins to DNA nanostructures, four commonly used structural motifs were tested: 1) a DNA duplex, 2) a hairpin loop with the trisNTA modification located in the loop region (the trisNTA modification is internal rather than at the 5'-end of the oligonucleotide), 3) a nicked double helix and 4) a double-crossover (DX) tile. DX tiles are rigid structures containing two four-arm branch junctions<sup>[23]</sup> and are one of the most commonly used motifs in the construction of extended two-dimensional DNA arrays.<sup>[24]</sup>

The DNA motifs were incubated with NiSO<sub>4</sub> and GFP as described above (except that, in the case of the double crossover tile, the final DNA concentration was 4.8  $\mu\text{M}$ ). The corresponding SEC traces are shown in Figure 3. In each case the GFP and DNA peaks are shifted and elute earlier. (In the traces shown in Figure 3C and D, the DNA absorption peak corresponding to the DNA-GFP complex and the peak corresponding to the unbound excess DNA are unresolved because of the large size of these motifs and the relatively small shift caused by GFP bind-

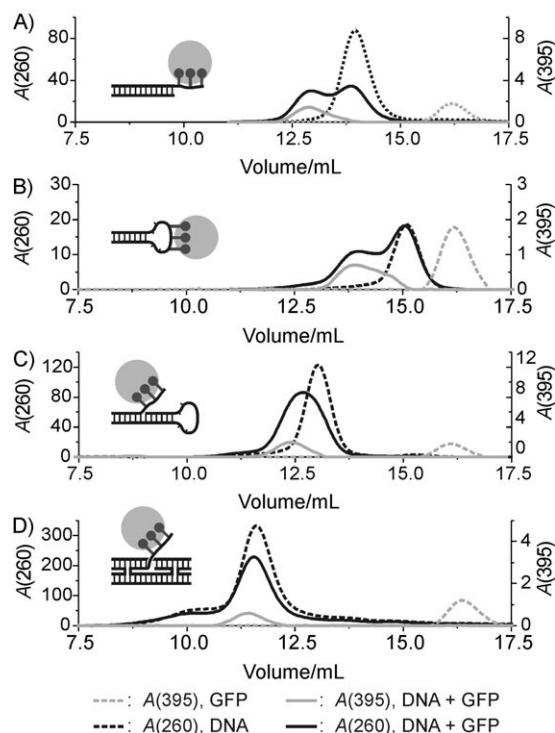


**Figure 3.** Binding of GFP to four different trisNTA-functionalized DNA nanostructure motifs (solid lines). A) Double-stranded DNA, B) hairpin loop with internal trisNTA modification, C) a nicked double helix and D) double-cross-over (DX) tile. Controls: DNA motifs only (dotted black lines); His<sub>6</sub>-tagged GFP only (dotted grey lines).

ing.) We conclude that all four DNA motifs bind GFP as expected.

### Equilibrium dissociation constant ( $K_D$ )

The equilibrium dissociation constant ( $K_D$ ) of the interaction between NTA-modified DNA and His<sub>6</sub>-tagged GFP was measured by titration (Table 2). A 27-mer DNA oligonucleotide con-

jugated to the fluorophore Cy3 at its 3'-end (Integrated DNA Technologies) was functionalized with mono-, bis- or trisNTA at the 5'-end, as described above. GFP and Cy3 form a weakly coupled FRET pair,<sup>[25]</sup> and GFP fluorescence is quenched in the proximity of nickel(II) ions.<sup>[26]</sup> His<sub>6</sub>-tagged GFP was titrated against the fluorescently labelled oligonucleotides with FRET as an indicator, and  $K_D$  was deduced by fitting the concentration-dependent binding probability (see the Experimental Section for details).

The measured  $K_D$  values are of the same order of magnitude as values previously obtained for binding between His<sub>6</sub>-tagged peptides or proteins and two or three NTA groups linked to fluorescent dye molecules<sup>[20,21]</sup> or biotin.<sup>[27]</sup> The trisNTA oligonucleotide has a very high affinity for the His<sub>6</sub>-tagged protein ( $K_D \sim 6$  nM). Based on a measurement of the association rate constant for a similar construct of  $10^{-5} \text{ M}^{-1} \text{ s}^{-1}$ ,<sup>[21]</sup> we estimate a dissociation rate constant of the order of  $10^{-3} \text{ s}^{-1}$ .

### Reversibility of binding

The linkage between trisNTA-modified DNA and a His<sub>6</sub>-tagged protein can be broken controllably by lowering the pH or by the addition of a competitor for the Ni<sup>2+</sup> coordination sites, for example ethylenediaminetetraacetic acid (EDTA; commonly used to elute His<sub>6</sub>-tagged proteins from Ni:NTA separation columns) or imidazole (data shown in the Supporting Information).

### Extended DNA arrays

We have also used the trisNTA modification to functionalize reversibly an extended two-dimensional DNA array with His<sub>6</sub>-tagged GFP. A DNA array with woven kagome architecture<sup>[2b]</sup> was formed by self-assembly. The unit cell of this array contains four different DNA oligonucleotides, one of which was functionalized such that the array carried a regular pattern of trisNTAs (Figure 4A). Arrays that were incubated with NiCl<sub>2</sub> and His<sub>6</sub>-tagged GFP were visible under a fluorescence microscope, thus indicating GFP binding (Figure 4B). Images of a control array in which one of the constituent oligonucleotides was co-

<b>Table 2.</b> Dissociation constants ( $K_D$ ) for binding between bis- and trisNTA-DNA and His <sub>6</sub> -tagged GFP measured by titration, with FRET as an indicator of binding. Published results for related constructs are included for comparison.		
bisNTA-DNA	trisNTA-DNA	Ref.
$0.12 \pm 0.03 \text{ } \mu\text{M}$	$0.006^{+0.004}_{-0.001} \text{ } \mu\text{M}$	
bisNTA-constructs	trisNTA-constructs	
$0.068 \pm 0.020 \text{ } \mu\text{M}$	$0.0021 \pm 0.0008 \text{ } \mu\text{M}$	21 <sup>[a]</sup>
$0.27 \pm 0.05 \text{ } \mu\text{M}$	$0.02 \pm 0.01 \text{ } \mu\text{M}$	21 <sup>[b]</sup>
–	$0.005 \text{ } \mu\text{M}$ (yCD)	27 <sup>[a]</sup>
–	$0.018\text{--}0.033 \text{ } \mu\text{M}$ (HIP1R)	27 <sup>[a]</sup>
$1.0 \text{ } \mu\text{M}$ (Cy3)	–	20 <sup>[c]</sup>
$0.4 \text{ } \mu\text{M}$ (Cy5)	–	20 <sup>[c]</sup>
$0.9 \text{ } \mu\text{M}$ (Cy3)	–	20 <sup>[d]</sup>
$0.3 \text{ } \mu\text{M}$ (Cy5)	–	20 <sup>[d]</sup>

[a]  $K_D$  deduced from measured association and dissociation rates. [b]  $K_D$  measured by isothermal titration calorimetry. [c]  $K_D$  measured by titration with fluorescence anisotropy as an indicator of binding. [d]  $K_D$  measured by titration with FRET as an indicator of binding.

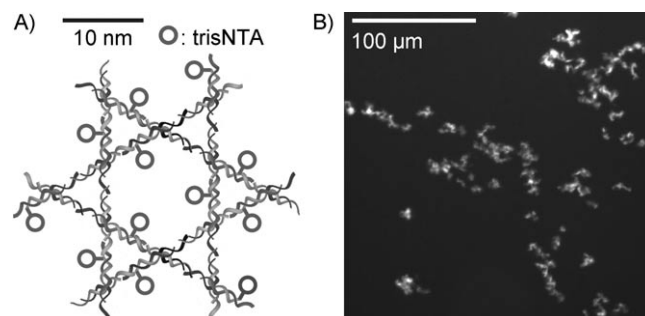


**Figure 4.** Decorating a DNA array with His<sub>6</sub>-tagged GFP. A) A section of the extended trisNTA-modified DNA kagome array. The 5'-end of one of the four constituent oligonucleotides is modified with trisNTA (indicated by a circle). B) Fluorescence microscopy image of an array with NTA modification + NiCl<sub>2</sub> + GFP. (Control experiments are shown in the Supporting Information.)



valently linked to the fluorescent dye Cy5 were similar, while no fluorescent arrays were seen in controls lacking NTA modification or nickel. Arrays decorated with GFP lose their fluorescence after being washed with the chelator imidazole, and regain fluorescence after the removal of imidazole and recharging the array with  $\text{NiCl}_2$  and GFP. (Data shown in the Supporting Information.)

## Conclusions

We have presented a new method for linking proteins to DNA. The required trisNTA-modified DNA is easily synthesised and purified. The linkage to a His<sub>6</sub>-tagged protein is formed by incubation at room temperature and can be broken controllably by addition of the competitors EDTA or imidazole and then reformed simply by removal of the competitor and reincubation with nickel ions and His<sub>6</sub>-tagged protein. We have demonstrated binding of His<sub>6</sub>-tagged GFP to a number of trisNTA-functionalized DNA motifs, including a DX tile, a hairpin with an internal trisNTA modification and an extended two-dimensional DNA array. The combination of low dissociation constant and reversibility of the linkage, its applicability to the broad class of His<sub>6</sub>-tagged recombinant proteins without the need for additional chemical modification and the mild reaction conditions make this linker particularly suitable for the creation of functional nanostructures by using self-assembled DNA architectures to position protein molecules.

## Experimental Section

### Synthesis

**Synthesis of NTA-modified oligonucleotides:** DNA oligos with one, two or three C<sub>6</sub>-amine modifications (Uni-Link™ amino modifiers, Clontech, supplied by Integrated DNA Technologies) were dissolved in H<sub>2</sub>O (to concentrations between 0.2 and 1 mM) and desalted by transferring the solution into phosphate buffer (100 mM sodium phosphate, 100 mM NaCl, pH 7.3) using a size-exclusion spin column (Bio-Rad, Micro Bio-Spin 6). DNA solution (50  $\mu\text{L}$ ) was combined with freshly dissolved SPDP (Sigma–Aldrich; 12.5  $\mu\text{L}$ , 50–100 mM in DMSO). After the mixture had been incubated for 1 h at room temperature, excess SPDP was removed by using a size-exclusion spin column that had been washed with phosphate buffer. TCEP (Tris(2-carboxyethyl)phosphine hydrochloride; Sigma–Aldrich; 6.25  $\mu\text{L}$ , ~100 mM) was added, and the mixture was incubated for 15 min at room temperature to reduce the disulfide bonds of SPDP. Maleimide–NTA (Dojindo, Kumamoto, Japan) was dissolved in phosphate buffer (50 mg mL<sup>-1</sup>). The maleimide–NTA solution (7  $\mu\text{L}$ ) was added to the DNA solution, and the mixture was incubated for 1 h at room temperature. (The molar excess of maleimide–NTA over DNA ranges from ~14:1 to ~70:1, depending on the initial DNA concentration.) Excess maleimide was removed by transferring the sample into HEPES (20 mM HEPES, 150 mM NaCl, pH 7.5) or phosphate buffer by using a spin column. The samples were then stored at 4 °C.

**Synthesis of controls:** Control experiments were performed on a substoichiometric amount of SPDP, so that not all amine modifications on all oligos could carry an NTA modification. Desalted DNA (5  $\mu\text{L}$ , 0.2 mM) carrying one, two or three amine modifications was combined with SPDP (1.25  $\mu\text{L}$ ) such that the molar ratio of amine

groups to SPDP was ~2:1. After incubation for 1 h at room temperature, phosphate buffer was added (10  $\mu\text{L}$ ), and the sample was passed through a spin column into phosphate buffer.  $\frac{1}{10}$ th volume TCEP (85 mM) was added, and the mixture was incubated for 15 min at room temperature, followed by addition of  $\frac{1}{10}$ th volume maleimide–NTA (100 mM) and incubation for 1 h. Excess maleimide–NTA was removed by transferring the sample into HEPES buffer on a spin column.

**Yield:** The yield of synthesis was estimated from band intensities in PAGE gels (see below) by using a Pharos FX Plus Molecular Imager and Quantity One analysis software (Bio-Rad).

**Purification and analysis by PAGE:** NTA-modified oligos can be purified from unmodified oligos by PAGE. The monoNTA sample shown in Figure 1 was PAGE purified. To resolve modified and unmodified oligos, samples were run on a two-layered, high-percentage denaturing gel with a discontinuous Tris–glycine buffer system<sup>[28]</sup> without SDS, but with urea (7 M) in the gels: stacking gel (0.84 g urea, 250  $\mu\text{L}$  Tris (1.0 M, pH 6.8), 330  $\mu\text{L}$  acrylamide/bis-acrylamide (29:1, 30%), brought up to 2 mL with deionized water); separating gel (2.1 g urea, 0.65 mL Tris (3 M, pH 8.8), 2.75 mL acrylamide/bis-acrylamide (19:1, 40%), brought up to 5 mL with deionized water); loading buffer (0.48 g urea, 93.75  $\mu\text{L}$ , 1.0 M Tris, pH 6.8, 62.5  $\mu\text{L}$  1% bromophenol blue dye, brought up to 1 mL with deionized water); running buffer (2.5 mM Tris, 0.19 M glycine). Samples were combined 1:1 with the loading buffer and heated to 95 °C for 5 min before being run on the gel. Gels were run at room temperature. A voltage of 150 V was applied for ~10 min (while the sample was migrating through the stacking layer) and then increased to ~300 V. DNA to be analysed was visualized by using silver stain (Figure 1) or SYBR Gold (Invitrogen). DNA to be purified was visualized by UV shadowing, and the desired band was cut out of the gel and recovered by using the crush-and-soak method: gel slices were transferred into a reaction vessel, crushed, covered with buffer, soaked overnight and spun on Millipore Ultrafree-MC HV centrifugal filters (0.45  $\mu\text{m}$ ) to remove gel fragments.

**Purification by reversed-phase liquid chromatography:** NTA-modified oligos can also be purified from unmodified oligos by using RPLC. The bis- and trisNTA samples shown in Figure 1 were RPLC purified on a GE Healthcare  $\mu\text{RPC C2/C18 ST 4.6}$  reversed-phase column with a volume (CV) of 1.7 mL. The column was connected to an ÄKTAbasic LC system and a Frac-920 fraction collector. The following buffers were used to purify NTA-modified oligos: buffer A: 0.1 M triethylammonium acetate, 5% acetonitrile; buffer B: 0.1 M triethylammonium acetate, 70% acetonitrile. The following buffer mixtures were pumped through the column at 0.5 mL min<sup>-1</sup>: 100% buffer A, 0% buffer B (2 CV); raise buffer B to 13% over 1 CV; 87% buffer A, 13% buffer B (8 CV); raise buffer B to 16% over 30 CV; raise buffer B to 100% over 1 CV. The oligonucleotides that were analysed by mass spectrometry (see below) were purified by RPLC on a Waters XBridge™ OST C18 column (2.5  $\mu\text{m}$  particle size, 4.6  $\times$  50 mm). The column was connected to an Agilent 1200 series LC system. The column was heated to 40 °C, and the flow rate was set to 1 mL min<sup>-1</sup>: 100% buffer A (5 min); raise buffer B to 16% over 18 min; raise buffer B to 100% over 4 min; 100% buffer B (3 min).

**Mass spectrometry:** NTA-modified oligos were prepared and purified by RPLC, as described above. The collected fractions were dried, resuspended in water and then passed through a size-exclusion spin column (Bio-Rad, Micro Bio-Spin 6) into water. EDTA was added to give a final DNA concentration of 5–8  $\mu\text{M}$  and a final EDTA concentration of 250–360  $\mu\text{M}$ . Liquid chromatography–mass

spectrometry (LC-MS) analysis was performed on an HP1050 LC coupled to a LCT Premier reflectron TOF mass spectrometer (Waters). Chromatography was carried out on a Waters XBridge OST C18 column (2.5  $\mu\text{m}$  particle size, 4.6 $\times$ 50 mm), with a linear gradient from 90% buffer C (400 mM 1,1,1,3,3,3-hexafluoroisopropanol, 16.3 mM triethylamine, 5% methanol)+10% buffer D (400 mM 1,1,1,3,3,3-hexafluoroisopropanol, 16.3 mM triethylamine, 60% methanol) to 30% buffer C+70% buffer D over 8 min. The eluent was directly injected into the mass spectrometer, and the data were acquired in the negative-ion mode (mass range 505–3500) and analyzed by using the manufacturer's software (MassLynx V4.1, Waters).

**Size-exclusion liquid chromatography:** Analytical size-exclusion liquid chromatography (SEC) was performed on a GE Healthcare Superdex 200 10/300 GL column (CV=23.6 mL), connected to an ÄKTA basic LC system, with TN buffer (10 mM Tris, 100 mM NaCl, pH 8) and a flow rate of 0.5 mL min<sup>-1</sup>. All SEC traces were processed by using the GE Healthcare UNICORN software package to subtract baselines and smooth.

**Formation of DNA motifs:** NTA-modified DNA motifs were assembled in TN buffer as follows. DNA duplexes were formed by combining the NTA-modified 27-mer "Oligo 1" with a 5–10% excess of a fully complementary, unmodified 27-mer (Oligo 2) and diluting it to a concentration of ~5.4  $\mu\text{M}$  in TN buffer (70  $\mu\text{L}$ ). The sample was heated to 50 °C for 10 min and then left to cool to room temperature. DNA hairpins were formed by heating Oligo 3 to 95 °C followed by rapid cooling to 4 °C. A nicked duplex was formed by combining Oligo 1 and Oligo 4, heating them to 95 °C and then allowing them to cool to room temperature. A double-crossover tile (DX tile)<sup>[23]</sup> was formed by combining the five component oligonucleotides (6  $\mu\text{M}$  final concentration), heating them to 95 °C and then allowing them to cool to room temperature over approximately 20 min. (The base sequences of all oligonucleotides are given in the Supporting Information.)

#### Measurement of the equilibrium dissociation constant ( $K_D$ )

**FRET and fluorescence quenching:** The fluorescence intensity of wild-type GFP ( $\lambda_{\text{ex max}}$  at 504 nm) is reduced, and the fluorescence intensity of Cy3 (average of 558–564 nm) is increased when photo-excited His<sub>6</sub>-GFP is bound to NTA-modified DNA labelled with a Cy3 fluorophore. Two effects contribute to these observations: GFP and Cy3 form a FRET pair,<sup>[25]</sup> and GFP fluorescence is quenched in the proximity of Ni<sup>2+</sup> cations.<sup>[26]</sup> Changes in the intensities of these two fluorescence bands can therefore be used to deduce changes in the relative concentrations of free DNA, free GFP and the DNA–GFP complex, when His<sub>6</sub>-GFP is titrated against Ni<sup>2+</sup><sub>2</sub>:bisNTA–DNA or Ni<sup>2+</sup><sub>3</sub>:trisNTA–DNA. The equilibrium dissociation constant ( $K_D$ ) can be deduced from these measurements.

**Materials:** Mono-, bis- and trisNTA-modified, Cy3-labelled Oligo 1 was prepared as described above from oligonucleotides carrying amine modifications at their 5'-end and a Cy3 modification at their 3'-end. The concentrations of stock solutions of NTA-modified DNA were determined by measuring absorbance (Nanodrop ND-1000) at 260 and 550 nm (Cy3 absorption). The concentration of His<sub>6</sub>-GFP (US Biological, Marblehead, MA, USA) was determined by measuring absorbance at 395 nm. The contribution of absorption by Cy3 at 260 nm was taken into account when calculating the DNA concentration. NTA-modified DNA was loaded with Ni<sup>2+</sup> by addition of NiCl<sub>2</sub> and diluted in buffer G (20 mM HEPES, pH 7.3, 137 mM NaCl, 20 mM KCl, 0.1% BSA, 5% glycerol) to give final concentrations of 3.14  $\mu\text{M}$  for bisNTA DNA and 7  $\mu\text{M}$  for NiCl<sub>2</sub>. The final concentrations in the trisNTA–DNA titration were 1.22  $\mu\text{M}$  of trisNTA–DNA

and 4  $\mu\text{M}$  of NiCl<sub>2</sub>. His<sub>6</sub>-GFP was diluted in buffer G to the desired initial concentration for titration (0.26 and 0.11  $\mu\text{M}$  for titration with Ni<sup>2+</sup><sub>2</sub>:bisNTA–DNA and Ni<sup>2+</sup><sub>3</sub>:trisNTA–DNA, respectively).

**Fluorescence measurements:** For the titration, GFP solution (60  $\mu\text{L}$ ) was placed in a quartz cuvette, and fluorescence spectra were measured by using a scanning fluorimeter (Photon Technology International, Birmingham, NJ, USA) with  $\lambda_{\text{ex}}$ =395 nm. Directly excited fluorescence of Cy3 in the absence of GFP is negligible; the fluorescence intensity at 504 nm is therefore the sum of terms proportional to the concentrations of free and bound His<sub>6</sub>-GFP. GFP fluorescence coinciding with the Cy3 band (558–564 nm) was assumed to be proportional to fluorescence at the GFP peak (504 nm) and was subtracted from the measured intensity in this band. The corrected intensity is proportional to the concentration of bound GFP.

**Titration:** Intensities of GFP and Cy3 fluorescence were measured during titrations of His<sub>6</sub>-GFP against Ni<sup>2+</sup><sub>2</sub>:bisNTA–DNA and Ni<sup>2+</sup><sub>3</sub>:trisNTA–DNA. (Cy3 fluorescence in the GFP band was subtracted.) Fits were performed with two adjustable parameters corresponding to  $K_D$  and to an overall proportionality constant relating the change in concentration of the complexes to the change in fluorescence intensity due to the formation of the complexes. The final determined value of  $K_D$  is the average of the fits to five independent titrations. The error is the sum of squares of the random error and an asymmetric, systematic error based on estimates of the uncertainty of the initial concentrations of DNA and GFP. (Fluorescence spectra and titration curves are shown in the Supporting Information.)

**Control experiments:** Control experiments were carried out to assess the importance of nonspecific interactions. No significant quenching of fluorescence from His<sub>6</sub>-GFP was observed upon addition of up to 20  $\mu\text{L}$  of NiCl<sub>2</sub> (7  $\mu\text{M}$ ) in the absence of DNA. In the absence of nickel ions, no significant change in GFP fluorescence was detected upon addition of up to 6  $\mu\text{L}$  of trisNTA–DNA (3.14  $\mu\text{M}$ ) or 14  $\mu\text{L}$  of bisNTA–DNA to 60  $\mu\text{L}$  of His<sub>6</sub>-GFP (0.26  $\mu\text{M}$ ). These concentrations were similar to the concentrations used for the actual titration. We deduce that titrations used to determine  $K_D$  for these constructs were not affected by nonspecific binding. However, addition of 15  $\mu\text{L}$  of monoNTA DNA (67  $\mu\text{M}$ ) to 60  $\mu\text{L}$  of GFP (4.9  $\mu\text{M}$ ) in the absence of nickel caused significant quenching of GFP fluorescence; this indicates that nonspecific binding is comparable in strength to the designed nickel-mediated interaction for monoNTA ( $K_D > 10 \mu\text{M}$ ).<sup>[20,21]</sup> No attempt was made to quantify the strength of nickel-mediated binding of monoNTA–DNA.

**Controlled breaking of the DNA–GFP linkage:** The linkage between trisNTA-modified DNA and a His<sub>6</sub>-tagged protein can be broken controllably by the addition of a competitor for the Ni<sup>2+</sup> coordination sites, for example, ethylenediaminetetraacetic acid (EDTA; commonly used to elute His<sub>6</sub>-tagged proteins from Ni:NTA separation columns) or imidazole, or by lowering pH. The trisNTA-functionalized DNA hairpin motif was incubated with NiSO<sub>4</sub> and His<sub>6</sub>-tagged GFP, as described above, to give the GFP–His<sub>6</sub>:Ni<sup>2+</sup><sub>3</sub>:trisNTA–DNA complex. Subsequent incubation with the chelating agent EDTA (10 mM final concentration, i.e., 1000-fold excess of EDTA over GFP) caused the complex to dissociate.

#### Fluorescence microscopy

**Coverslip silanization and construction of "tunnel slide":** Glass coverslips were cleaned by immersion in saturated aqueous KOH for ~12 h, sonication for ~1 h and thorough rinsing with distilled water. They were then silanized by immersion in ethanol contain-

ing 0.02% (v/v) acetic acid and 2% (v/v) 3-mercaptopropyltrimethoxysilane (MPS) heated to  $\sim 70^{\circ}\text{C}$ , in a hot water bath for  $\sim 2$  h. Finally, the coverslips were washed thoroughly with distilled water and placed in an oven set to  $120^{\circ}\text{C}$  for  $\sim 30$  min. A tunnel ( $\sim 5\ \mu\text{L}$ ) was formed between two parallel strips of double-sided sticky tape, a silanized coverslip and a glass microscope slide.

**Formation and immobilization of 2-D DNA arrays:** TrisNTA-kagome arrays<sup>[2b]</sup> were formed by cooling four oligonucleotides (at a concentration of  $3\ \mu\text{M}$ ) from  $90$  to  $10^{\circ}\text{C}$  over  $65$  h in  $\text{MgCl}_2$  ( $30\ \text{mM}$ ) and Tris-HCl ( $20\ \text{mM}$ , pH 8.8) by using a Mastercycler PCR machine (Eppendorf). The arrays were immobilized onto coverslip surfaces by incubating array solutions within separate tunnel slides for  $\sim 10$  min at  $20^{\circ}\text{C}$ .

**Binding assay and fluorescence microscopy:** Nonimmobilized arrays were washed off the coverslip surfaces with four washes ( $10\ \mu\text{L}$ ) of buffer F ( $30\ \text{mM}$   $\text{MgCl}_2$ ,  $20\ \text{mM}$  Tris-HCl pH 8.8). The tunnel slide was then incubated with  $\sim 10\ \mu\text{L}$  of GFP incubation buffer ( $7\ \mu\text{M}$  His<sub>6</sub>-tagged GFP,  $1\ \text{mg mL}^{-1}$  bovine serum albumin (BSA),  $100\ \text{mM}$  NaCl, buffer F for  $5$  min at  $20^{\circ}\text{C}$ . After washes with buffer F ( $4 \times 10\ \mu\text{L}$ ), fluorescence images were recorded, and no fluorescence was observed (see the Supporting Information). Nickel(II) ions were supplied by washing with buffer E ( $2 \times 10\ \mu\text{L}$ ;  $10\ \text{mM}$   $\text{NiCl}_2$ , buffer F) and incubating with buffer E for  $\sim 5$  min at  $20^{\circ}\text{C}$ . Excess  $\text{Ni}^{2+}$  was removed by flushing with buffer F ( $4 \times 10\ \mu\text{L}$ ). The slide was then reincubated with GFP incubation buffer ( $\sim 10\ \mu\text{L}$ ) for  $5$  min at  $20^{\circ}\text{C}$ . Excess GFP was removed with buffer F ( $4 \times 10\ \mu\text{L}$ ). The fluorescence image shown in Figure 4B was then recorded. (See the Supporting Information for control experiments and a demonstration of reversible binding between GFP and the DNA arrays.) Tunnel slides were illuminated with a mercury source lamp (Olympus) and imaged by using an Andor Ixon CCD (Andor Technology, Belfast, UK) on an inverted IX71 Olympus optical microscope (Olympus).

## Acknowledgements

This work was supported by the UK research councils BBSRC, EPSRC and MRC, and by the MoD through the UK Bionanotechnology IRC. We are grateful for assistance from Konstantinos Lymperopoulos and Mike Heilemann.

**Keywords:** DNA • nanostructures • nanotechnology • proteins • self-assembly

- [1] a) H. Y. Li, S. H. Park, J. H. Reif, T. H. LaBean, H. Yan, *J. Am. Chem. Soc.* **2004**, *126*, 418–419; b) Y. Liu, C. X. Lin, H. Y. Li, H. Yan, *Angew. Chem.* **2005**, *117*, 4407–4412; *Angew. Chem. Int. Ed.* **2005**, *44*, 4333–4338.
- [2] a) H. Yan, S. H. Park, G. Finkelstein, J. H. Reif, T. H. LaBean, *Science* **2003**, *301*, 1882–1884; b) J. Malo, J. C. Mitchell, C. Vénien-Bryan, J. R. Harris, H. Wille, D. J. Sherratt, A. J. Turberfield, *Angew. Chem.* **2005**, *117*, 3117–3121; *Angew. Chem. Int. Ed.* **2005**, *44*, 3057–3061.
- [3] B. P. Duckworth, Y. Chen, J. W. Wollack, Y. Sham, J. D. Mueller, T. A. Taton, M. D. Distefano, *Angew. Chem.* **2007**, *119*, 8975–8978; *Angew. Chem. Int. Ed.* **2007**, *46*, 8819–8822.
- [4] C. M. Erben, R. P. Goodman, A. J. Turberfield, *Angew. Chem.* **2006**, *118*, 7574–7577; *Angew. Chem. Int. Ed.* **2006**, *45*, 7414–7417.
- [5] C. M. Niemeyer, J. Koehler, C. Wuerdemann, *ChemBioChem* **2002**, *3*, 242–245.
- [6] a) F. Kukulka, B. K. Müller, S. Paternoster, A. Arndt, C. M. Niemeyer, C. Bräuchle, D. C. Lamb, *Small* **2006**, *2*, 1083–1089; b) F. Kukulka, O. Schöps, U. Woggon, C. M. Niemeyer, *Bioconjugate Chem.* **2007**, *18*, 621–627; c) H. Lu, O. Schöps, U. Woggon, C. M. Niemeyer, *J. Am. Chem. Soc.* **2008**, *130*, 4815–4827.
- [7] a) T. Sano, C. L. Smith, C. R. Cantor, *Science* **1992**, *258*, 120–122; b) C. M. Niemeyer, M. Adler, R. Wacker, *Nat. Protocols* **2007**, *2*, 1918–1930.
- [8] C. M. Niemeyer, T. Sano, C. L. Smith, C. R. Cantor, *Nucleic Acids Res.* **1994**, *22*, 5530–5539.
- [9] S. S. Ghosh, P. M. Kao, A. W. McCue, H. L. Chappelle, *Bioconjugate Chem.* **1990**, *1*, 71–76.
- [10] D. R. Corey, P. G. Schultz, *Science* **1987**, *238*, 1401–1403.
- [11] S. S. Smith, L. M. Niu, D. J. Baker, J. A. Wendel, S. E. Kane, D. S. Joy, *Proc. Natl. Acad. Sci. USA* **1997**, *94*, 2162–2167.
- [12] a) S. Takeda, S. Tsukiji, T. Nagamune, *Bioorg. Med. Chem. Lett.* **2004**, *14*, 2407–2410; b) M. Lovrinovic, M. Spengler, C. Deutsch, C. M. Niemeyer, *Mol. Biosyst.* **2005**, *1*, 64–69.
- [13] a) A. D. Ellington, J. W. Szostak, *Nature* **1990**, *346*, 818–822; b) L. C. Bock, L. C. Griffin, J. A. Latham, E. H. Vermaas, J. J. Toole, *Nature* **1992**, *355*, 564–566.
- [14] C. X. Lin, E. Katilius, Y. Liu, J. P. Zhang, H. Yan, *Angew. Chem.* **2006**, *118*, 5422–5427; *Angew. Chem. Int. Ed.* **2006**, *45*, 5296–5301.
- [15] Y. He, Y. Tian, A. E. Ribbe, C. D. Mao, *J. Am. Chem. Soc.* **2006**, *128*, 12664–12665.
- [16] a) P. Simon, C. Dueymes, M. Fontecave, J.-L. Décout, *Angew. Chem.* **2005**, *117*, 2824–2827; *Angew. Chem. Int. Ed.* **2005**, *44*, 2764–2767; b) L. Fruk, C. M. Niemeyer, *Angew. Chem.* **2005**, *117*, 2659–2662; *Angew. Chem. Int. Ed.* **2005**, *44*, 2603–2606.
- [17] N. M. Green, *Methods Enzymol.* **1990**, *184*, 51–67.
- [18] C. M. Niemeyer, M. Adler, B. Pignataro, S. Lenhart, S. Gao, L. F. Chi, H. Fuchs, D. Blohm, *Nucleic Acids Res.* **1999**, *27*, 4553–4561.
- [19] a) E. Hochuli, H. Döbeli, A. Schacher, *J. Chromatogr.* **1987**, *411*, 177–184; b) E. Hochuli, W. Bannwarth, H. Döbeli, R. Gentz, D. Stüber, *Bio/Technology* **1988**, *6*, 1321–1325.
- [20] A. N. Kapanidis, Y. W. Ebricht, R. H. Ebricht, *J. Am. Chem. Soc.* **2001**, *123*, 12123–12125.
- [21] S. Lata, A. Reichel, R. Brock, R. Tampé, J. Piehler, *J. Am. Chem. Soc.* **2005**, *127*, 10205–10215.
- [22] R. Heim, D. C. Prasher, R. Y. Tsien, *Proc. Natl. Acad. Sci. USA* **1994**, *91*, 12501–12504.
- [23] T.-J. Fu, N. C. Seeman, *Biochemistry* **1993**, *32*, 3211–3220.
- [24] E. Winfree, F. R. Liu, L. A. Wenzler, N. C. Seeman, *Nature* **1998**, *394*, 539–544.
- [25] Y. Suzuki, *Methods* **2000**, *22*, 355–363.
- [26] a) J. A. Kemlo, T. M. Shepherd, *Chem. Phys. Lett.* **1977**, *47*, 158–162; b) A. Torrado, G. K. Walkup, B. Imperiali, *J. Am. Chem. Soc.* **1998**, *120*, 609–610; c) T. A. Richmond, T. T. Takahashi, R. Shimkhada, J. Bernsdorf, *Biochem. Biophys. Res. Commun.* **2000**, *268*, 462–465.
- [27] Z. H. Huang, J. I. Park, D. S. Watson, P. Hwang, F. C. Szoka, *Bioconjugate Chem.* **2006**, *17*, 1592–1600.
- [28] U. K. Laemmli, *Nature* **1970**, *227*, 680–685.

Received: March 23, 2009

Published online on May 15, 2009